

# Magnetic-field-induced Heisenberg to XY crossover in a quasi-2D quantum antiferromagnet

N A Fortune<sup>1</sup>, S T Hannahs<sup>2</sup>, C P Landee<sup>3</sup>, M M Turnbull<sup>4</sup>, F Xiao<sup>5</sup>

<sup>1</sup> Department of Physics, Smith College, Northampton MA, USA

<sup>2</sup> National High Magnetic Field Laboratory, Florida State University, Tallahassee FL, USA

<sup>3</sup> Department of Physics, Clark University, Worcester MA, USA

<sup>4</sup> Department of Chemistry, Clark University, Worcester MA, USA

<sup>5</sup> Department of Physics, Durham University, Durham, UK

E-mail: nfortune@smith.edu

**Abstract.** The magnetic-field-dependent ordering temperature of the quasi-2D quantum Heisenberg antiferromagnet (QHAF)  $\text{Cu}(\text{pz})_2(\text{ClO}_4)_2$  was determined by calorimetric measurement in applied dc fields up to 33 tesla. The magnetic phase diagram shows a round maximum at 5.95 K and 17.5 T (at  $\approx 1/3$  of its saturation field), a 40 percent enhancement of the ordering temperature above the zero field value of 4.25 K. The enhancement and reentrance are consistent with predictions of a field-induced Heisenberg to XY crossover behavior for an ideal 2D QHAF system.

## 1. Introduction

The copper pyrazine (pz)-based antiferromagnet  $\text{Cu}(\text{pz})_2(\text{ClO}_4)_2$  is a quasi-2D  $S = \frac{1}{2}$  square-lattice quantum Heisenberg antiferromagnet with weak intraplanar anisotropy. As shown in Figure 1 the Cu ions are connected within an a-b layer via pyrazine (pz) molecules [1]; adjacent layers are offset along the crystal a and b axes, resulting in an even weaker interlayer exchange interaction (on the order of  $J/J' < 10^{-4}$ ). With a similar structure to the square-lattice copper-oxides, but much smaller interaction strengths and saturation fields ( $\mu_0 H = 48$  T), molecular magnets such as  $\text{Cu}(\text{pz})_2(\text{ClO}_4)_2$  can be used to study the 2D Quantum Heisenberg antiferromagnet (QHAF) in the strong field limit.

Quantum fluctuations act to suppress magnetic order. An ideal Heisenberg square lattice antiferromagnet orders only at  $T = 0$  — with an expected magnetic moment of  $0.6\mu_B$  — but weak interplanar coupling and/or small XY anisotropy can reduce the magnitude of the quantum fluctuations, stabilizing Néel-type antiferromagnetic ordering at temperatures above zero K in zero field [2, 3]. In the case of  $\text{Cu}(\text{pz})_2(\text{ClO}_4)_2$ , long range 3D magnetic order occurs at  $T_N = 4.25$  K in zero field. Evidence for the suppression of magnetic ordering by quantum fluctuations is seen in both the reduced magnetic moment of  $0.47\mu_B$  per  $\text{Cu}^{2+}$  ion at  $T \rightarrow 0$  in zero field and in the surprising increase of  $T_N$  in an applied magnetic field. The increase is attributed to field-induced suppressions of those fluctuations [4].

Interestingly, the low-field susceptibility [2] shows evidence of an exchange-anisotropy crossover from Heisenberg to XY-like behavior just above  $T_N$ , as shown in Figure 2. The crossover from Heisenberg to XY anisotropy is taken to occur at  $T_{\min}$ , the minimum in the  $\chi_z$



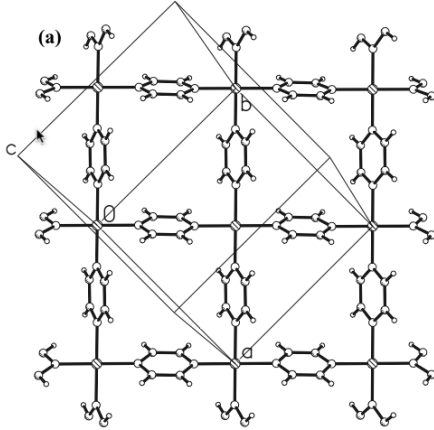


**Figure 1.**  $\text{Cu}(\text{Pz})_2(\text{ClO}_4)_2$  crystal structure (as viewed  $\perp$  ab plane). Cu ions are connected within a layer via pyrazine (pz) molecules.  $\text{ClO}_4$  ions not shown. Adjacent layers are offset along a and b, leading to a very weak interlayer exchange interaction  $J'$ .

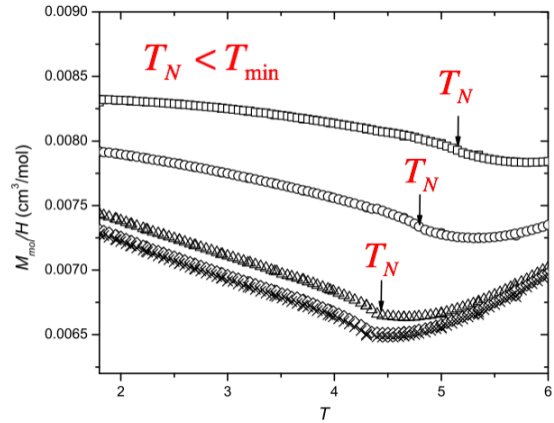


**Figure 2.**  $\chi_z$  for weak fields of 1 to 50 kOe applied  $\perp$  to layers (from Ref. [2]). As temperature decreases, the out of plane susceptibility passes through a minimum at  $T_{\min}$ , followed by long range 3D order at  $T_N$ . The minimum is a signature of XY anisotropy.

versus  $T$  curve. 3D long range antiferromagnetic ordering occurs at  $T_N$  (where  $T_N < T_{\min}$ ), as confirmed by  $\mu^+\text{SR}$  [2]. This can be understood as follows: as the temperature decreases, the small amount of XY anisotropy in the system causes a larger proportion of spins to antialign in the xy plane, thereby increasing the fraction of antiferromagnetic coupled spins available to cant in the direction of an applied field along the z axis. The result is an increase in  $\chi_z$  with decreasing temperature at sufficiently low temperatures, as observed. Like  $T_N$ , the crossover temperature  $T_{\min}$  also increases with increasing field.

## 2. Model Hamiltonian

In the simplest model Hamiltonian that can capture this physics,

$$H = J \sum_{nn} [S_i^x S_j^x + S_i^y S_j^y + (1 - \Delta) S_i^z S_j^z] + J' \sum_{i,i'} \mathbf{S}_i \cdot \mathbf{S}_{i'} - g\mu_B\mu_0 \mathbf{H} \cdot \sum_j \mathbf{S}_j \quad (1)$$

where the first summation is over nearest neighbors, the second summation links each spin to its counterparts in adjacent layers, and the third summation includes all spins.  $J$  is the intraplanar nearest-neighbor coupling strength,  $J'$  is the effective interplanar coupling strength, and  $\Delta$  is an exchange anisotropy parameter. For an ideal 2D quantum Heisenberg antiferromagnet,  $J' = 0$  and  $\Delta = 0$ , whereas for an ideal 2D XY model,  $J' = 0$  and  $\Delta = 1$ . The actual values of  $J$ ,  $J'$ , and  $\Delta$  must be experimentally determined.

The addition of weak antiferromagnetic next-nearest-neighbor interactions are expected to dramatically increase quantum fluctuations, destabilizing the ordering in the antiferromagnet state [5]. Next nearest neighbor interactions are not explicitly included in Eq. 1, but in a 2D effective spin model (in which both the exchange anisotropy  $\Delta$  and interplanar coupling  $J'$  terms are taken to be zero), they can be approximated by replacing  $J$  with an effective value  $J_{\text{eff}} = J_1 - J_2$ , where  $J_1$  and  $J_2$  represent the strength of nearest neighbor (NN) and next nearest neighbor (NNN) calculations, respectively. Applying the effective spin model approximation to neutron inelastic scattering data [5] yields a estimate  $\frac{J_2}{J_1} \simeq 0.02$  for the relative strengths of the

next nearest neighbor and nearest neighbor terms. Given an experimentally inferred value of  $J_1 = 1.54\text{meV}$ , we then have  $J_{\text{eff}} = J_1 - J_2 = (0.98)J_1 = 1.51\text{ meV}$  (17.5 K).

New angle-dependent ESR data [3] suggests, however, that this choice of an XY model with single anisotropy parameter  $\Delta$  overlooks a weak in-plane anisotropy that is important for the low-field behavior, resulting in a spin-flop phase transition at 0.42 T (in the zero temperature limit) for magnetic fields applied along the easy axis. Ignoring interplanar coupling terms, a model Hamiltonian for this biaxial anisotropy becomes

$$H = J \sum_{i,j} [S_i^x S_j^x + (1 - \Delta_y) S_i^y S_j^y + (1 - \Delta_z) S_i^z S_j^z] - g\mu_B \mathbf{H} \cdot \sum_j \mathbf{S}_j \quad (2)$$

where the first term is a sum over nearest neighbors and the second term is a sum over all spins. Assuming a nearest neighbor coupling strength of  $J = 18.1\text{K}$  (1.56 meV), a fit to the data yields exchange-anisotropy values of  $\Delta_y = 3.1 \times 10^{-4}$  and  $\Delta_z = 3.1 \times 10^{-3}$  [3]. Interestingly, the in-plane anisotropy changes sign above the spin-flop transition (for fields directed along  $x$ ). Defining  $\delta_y \equiv J(1 - \Delta_y)$  and  $\delta_z \equiv J(1 - \Delta_z)$ , the ESR biaxial model yields values of  $\delta_y = 5.3\text{mK}$  and  $\delta_z = 53.2\text{mK}$  below the spin-flop-transition, while above the spin-flop transition,  $\delta_y^* = -6.7\text{mK}$ . In the calorimetric measurements presented here, however, the field was applied along the  $z$  axis rather than  $x$ ; we plan to investigate the low-field field-angle dependent behavior in the vicinity of the spin-flop transition in a future experiment.

Combining the two models to include both the intraplanar variation in the exchange anisotropy parameter  $\Delta$  and the interplanar coupling parameter  $J'$ ,

$$H = J \sum_{i,j} [S_i^x S_j^x + (1 - \Delta_y) S_i^y S_j^y + (1 - \Delta_z) S_i^z S_j^z] - g\mu_B \mathbf{H} \cdot \sum_j \mathbf{S}_j + J' \sum_{i,i'} \mathbf{S}_i \cdot \mathbf{S}_{i'} \quad (3)$$

where  $J = 18.1\text{K}$  and  $\Delta_z = 3.1 \times 10^{-3}$ , while  $\Delta_y = 3.1 \times 10^{-4}$  for fields directed along  $z$  and  $\Delta_y = -3.9 \times 10^{-4}$  for fields directed along  $x$ . This model Hamiltonian does not directly include contributions next nearest neighbors; one solution to this could be to replace  $J = 18.1\text{ K}$  with an effective  $J_{\text{eff}} = 17.5\text{ K}$  as before.

Because the interplanar coupling constant  $J'$  and anisotropy parameter  $\Delta$  (or  $\Delta_y$  and  $\Delta_z$ ) and their interplay determine so much of the physical behavior in these materials — including the zero-field-ordering temperature and the initial enhancement of antiferromagnetic ordering with field at low field — it is critical to obtain an accurate value for  $J'$  as well. Unfortunately, currently available theoretical models used to estimate  $J'$  from  $J$  and  $T_N$  [6] rely on the assumption that the exchange interactions are purely Heisenberg (and therefore assume  $\Delta = 0$ ).

One promising alternative is to experimentally determine  $J'$  and  $\Delta$  in a self-consistent manner from a numerical Quantum Monte Carlo (QMC) fit [7] to the magnetic-field-dependence of the antiferromagnetic phase boundary  $T_N(\mu_0 H)$ . In this paper we present the experimental data needed for such a calculation for  $\text{Cu}(\text{pz})_2(\text{ClO}_4)_2$ . QMC fits to the data using Eq. 1 and Eq. 3 are ongoing; the full results of these calculations will be presented in a later publication.

### 3. Experimental Methods and Results

For these measurements, we used a custom-built miniature sample-in-vacuum calorimeter [8] designed to fit inside the National High Magnetic Field Laboratory (NHMFL) top-loading dilution refrigerator single-axis rotating sample probes [9]. The calorimeter can be used for both ac calorimetric [10] and thermal-relaxation calorimetric [11] measurements in field.

Figure 3 shows the 1 mm x 1.3 mm x 0.3 mm thick  $\text{Cu}(\text{Pz})_2(\text{ClO}_4)_2$  sample (in blue) sandwiched between a low mass sample thermometer and sample heater. The sample thermometer and heater leads serve as the weak thermal link to a temperature-controlled silver/sapphire platform. The platform and sample assembly are in vacuum; the platform's

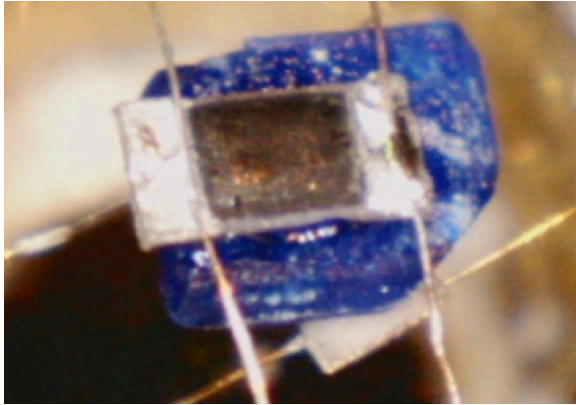


**Figure 3.**  $\text{Cu}(\text{Pz})_2(\text{ClO}_4)_2$  sample (blue) sandwiched between a sample thermometer and heater. The leads serve as the thermal link to a temperature-controlled platform.

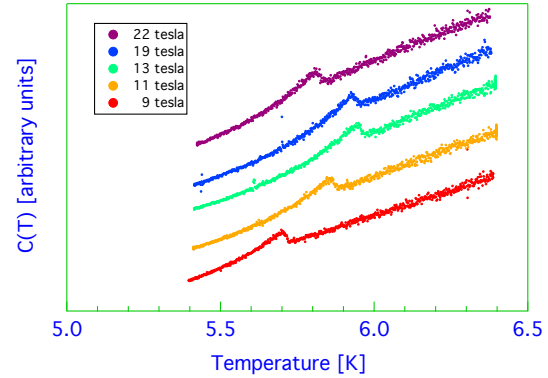


**Figure 4.** Heat capacity as a function of temperature for series of fixed magnetic fields near the peak of phase boundary at 5.95 K, 17.5 T. Curves offset for clarity.

supporting post and sensor leads provide a thermal link to the external cryogenic bath. The dependence of platform temperature on platform heater power is well described by the magnetic-field-independent power law function  $T = T_0 + A(P_0 + P)^n$  where  $n \lesssim 0.5$ .  $A$  and  $n$  depend only on the properties of the calorimeter;  $P_0$  and  $T_0$  also depend on the properties of the fridge.

After repeated thermal cycling, the thermometers were cross-calibrated in zero field against a commercially calibrated RuOx resistive thermometer. This data was used to fit the temperature dependence of each resistive sensor to the Chebyshev polynomial  $\log R(T, B) = \sum_{n=0}^N c_n(B) t_n(x)$  where  $x$  is a function of  $\log T$  [12]. A series of platform heater power sweeps in fixed magnetic fields (starting from the same refrigerator base temperature) then allowed us to fit the magnetic field dependence of  $c_n(B)$  as described in detail elsewhere [12].

In Figure 5 we present the measured ac-calorimetric response — which is inversely proportional to the heat capacity  $C(T/T_N)$  — for a series of field-corrected constant temperature field sweeps between 0 and 33 tesla. The entrances into and then out of the antiferromagnetic state are visible as dips in the ac-calorimetric response (peaks in heat capacity). The crossings of the phase boundary are plotted as a function of magnetic field and temperature in Figure 6. The ordering temperature  $T_N(\mu_0 H)$  increases by 40% in field, reaching a maximum of 5.95 K at 17.5 tesla. Similar re-entrant behavior has been reported for  $\text{Cu}(\text{HF}_2)(\text{pz})_2\text{BF}_4$  [13].

The experimentally observed field dependence of the phase boundary in  $\text{Cu}(\text{Pz})_2(\text{ClO}_4)_2$  is characteristic of the behavior expected for a magnetic-field-dependent Berezinskii-Kosterlitz-Thouless (BKT) transition in a 2D XY system with anisotropy  $\Delta$  [14, 15]. An idea 2D Quantum Heisenberg antiferromagnet (QHAF) with small XY anisotropy can also undergo a BKT transition, if it first undergoes a crossover from Heisenberg to XY behavior [16, 17]. The application of a magnetic field can also induce a Heisenberg to XY crossover and a finite temperature BKT transition  $T_{\text{BKT}}$  [4, 15]. For small fields, the reduction in quantum fluctuations of the z components of the spins dominates, leading to an increase of  $T_{\text{BKT}}$  with increasing field. At higher fields, the reduction in the XY spin moment due to spin-canting grows in importance, leading to a broad peak and then decline in  $T_{\text{BKT}}$  with increasing field [15].

An Initial QMC calculation [13] applying the field-dependent BKT model to the anisotropic quasi-2D QHAF system  $\text{Cu}(\text{HF}_2)(\text{pz})_2\text{BF}_4$  is promising, but this simplified calculation failed to take into account the XY anisotropy  $\Delta$ . A complete QMC calculation that includes both  $\Delta$  and  $J'$  is needed determine self-consistent values for these parameters and confirm the applicability of the general model to these materials.

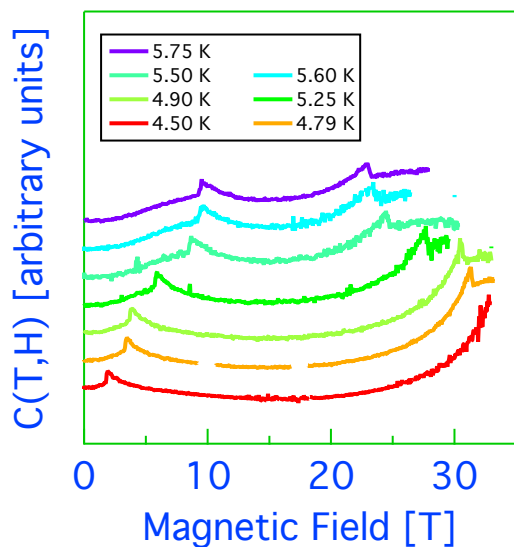


**Figure 5.** Heat capacity of  $\text{Cu}(\text{Pz})_2(\text{ClO}_4)_2$  as a function of magnetic field for series of fixed temperatures. Curves offset for clarity.

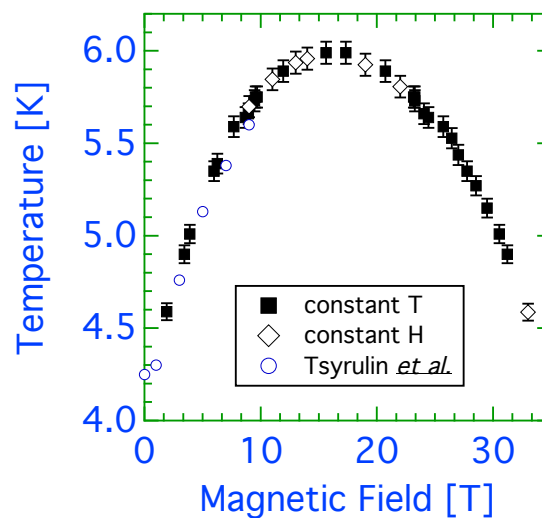


**Figure 6.** Field dependence of  $T_N$  from  $C(T,H)$ : this work and Tsyrlin *et al.* [4].

### Acknowledgments

A portion of this work was performed at the National High Magnetic Field Laboratory, which is supported by National Science Foundation Cooperative Agreement No. DMR-1157490, the State of Florida, and the U.S. Department of Energy.

### References

- [1] Woodward F M, Gibson P J, Jameson G B, Landee C P, Turnbull M M and Willett R D 2007 *Inorganic Chemistry* **46** 4256–4266
- [2] Xiao F, Woodward F, Landee C, Turnbull M, Mielke C, Harrison N, Lancaster T, Blundell S, Baker P, Babkevich P and Pratt F 2009 *Physical Review B* **79** 134412
- [3] Povarov K Y, Smirnov A I and Landee C P 2013 *Physical Review B* **87** 214402
- [4] Tsyrlin N, Xiao F, Schneidewind A, Link P, Ronnow H M, Gavilano J, Landee C P, Turnbull M M and Kenzelmann M 2010 *Physical Review B* **81** 134409
- [5] Tsyrlin N, Pardini T, Singh R, Xiao F, Link P, Schneidewind A, Hiess A, Landee C, Turnbull M and Kenzelmann M 2009 *Physical Review Letters* **102** 197201
- [6] Yasuda C, Todo S, Hukushima K, Alet F, Keller M, Troyer M and Takayama H 2005 *Physical Review Letters* **94** 217201
- [7] Bauer B *et al.* 2011 *Journal of Statistical Mechanics: Theory and Experiment* **2011** P05001
- [8] Hannahs S T and Fortune N A 2003 *Physica B-Condensed Matter* **329-333** 1586–1587
- [9] Palm E C and Murphy T P 1999 *Review Of Scientific Instruments* **70** 237–239
- [10] Sullivan P and Seidel G 1968 *Physical Review* **173** 679–685
- [11] Bachmann R *et al.* 1972 *Review Of Scientific Instruments* **43** 205–214
- [12] Fortune N A, Gossett G, Peabody L, Lehe K, Uji S and Aoki H 2000 *Review Of Scientific Instruments* **71** 3825–3830
- [13] Sengupta P *et al.* 2009 *Physical Review B* **79** 060409
- [14] Cuccoli A, Roscilde T, Vaia R and Verrucchi P 2003 *Physical Review Letters* **90** 167205
- [15] Cuccoli A, Roscilde T, Vaia R and Verrucchi P 2003 *Physical Review B* **68** 060402
- [16] Ding H 1992 *Physical Review Letters* **68** 1927–1930
- [17] Cuccoli A, Roscilde T, Tognetti V, Vaia R and Verrucchi P 2003 *Physical Review B* **67** 104414